

# Optics Letters

## Photonic hook: a new curved light beam

LIYANG YUE,<sup>1,\*</sup> OLEG V. MININ,<sup>2</sup> ZENGBO WANG,<sup>1</sup> JAMES N. MONKS,<sup>1</sup> ALEXANDER S. SHALIN,<sup>3</sup> AND IGOR V. MININ<sup>4,5</sup>

<sup>1</sup>School of Electronic Engineering, Bangor University, Dean Street, Bangor, Gwynedd, LL57 1UT, UK

<sup>2</sup>National Research Tomsk State University, Lenin Ave., 36, Tomsk 634050, Russia

<sup>3</sup>Nano-Optomechanics lab, ITMO University, 49 Kronverksky Ave., 197101, St. Petersburg, Russia

<sup>4</sup>National Research Tomsk Polytechnic University, Lenin Ave., 30, Tomsk 634050, Russia

<sup>5</sup>e-mail: prof.minin@gmail.com

\*Corresponding author: l.yue@bangor.ac.uk

Received 28 September 2017; revised 3 December 2017; accepted 10 January 2018; posted 12 January 2018 (Doc. ID 308158); published 9 February 2018

**It is well known that electromagnetic radiation propagates along a straight line, but this common sense was broken by the artificial curved light—the Airy beam. In this Letter, we demonstrate a new type of curved light beam besides the Airy beam, the so-called “photonic hook.” This photonic hook is a curved high-intensity focus by a dielectric trapezoid particle illuminated by a plane wave. The difference between the phase velocity and the interference of the waves inside the particle causes the phenomenon of focus bending.** © 2018 Optical Society of America

**OCIS codes:** (290.0290) Scattering; (260.2110) Electromagnetic optics; (050.1940) Diffraction; (230.0230) Optical devices.

<https://doi.org/10.1364/OL.43.000771>

The Airy waveform was first theorized as a solution to the Schrödinger equation by Berry and Balázs *et al.* in 1979 [1]. In 2007, Siviloglou *et al.* successfully observed an Airy beam in both one-/two-dimensional configurations [2]. As an Airy beam propagates, it will bend to form a parabolic arc in a medium, rather than diffract due to its uncommon beam profile (an area of principal intensity and less luminous areas to infinity) [2]. Unique properties of the Airy beam, e.g., free acceleration [3,4], self-healing [5], and a large field of view when forming a light sheet [6], have been reported in the generally acknowledged scientific literature, and afforded potentially important applications for imaging and manipulating microscale objects [6,7]. Meanwhile, a microparticle can act as a refractive micro-lens to focus the lightwave within a subwavelength volume [8,9]. This generates a narrow, highly intensive, weak-diverging beam known as a “photonic jet,” which propagates into the background medium from the shadow side of a particle [10,11].

To the best of our knowledge, there is no research published about the formation of curved photonic jets. In this Letter, we report a new way to produce the curved light beam, named “photonic hook” to emphasize its curvature characteristic [12]. The key difference between the photonic hook and

the Airy beam is that the photonic hook is created using the focusing of a plane wave through an asymmetric dielectric particle which is the combination of a wedge prism and a cuboid. This process should be simpler than the generation of an Airy beam using a laser and a spatial light modulator [2]. The formation of the photonic jet within the terahertz band in a symmetrically cuboid particle has been investigated in our previous publication [12]. Relying on the established knowledge, the influence of the size and prism angle of an asymmetric particle on the distribution of field enhancement, width (full-width at half-maximum [FWHM]), and curvature of the photonic hook is effectively quantified in this Letter.

The numerical model of a symmetric/asymmetric particle irradiated by a plane wave is built in the commercial finite integral technique software package—CST Microwave Studio. A 532 nm wavelength ( $\lambda$ ) plane wave propagates from  $+z$  to  $-z$  direction and is polarized along the  $y$ -axis. The model represents a dielectric cuboid with the addition of a wedge-shaped prism made of the same material on the face encountering plane wave, while the same sized cuboid without  $z$  prism is also simulated as a reference. The refractive indices of the particle material (transparent fused silica) and background medium (air) are set up to 1.46 and 1.0, respectively [13]. The cuboid structure has equal length, width, and height. Side length,  $L$ , is normalized to  $\lambda$ , and angle  $\alpha$  defines the inclined plane of the prism.

Figure 1(a) describes the  $E^2$  field enhancement distribution of the plane wave passing through the (1) symmetric and (2) asymmetric particles with  $L = 3\lambda$ . In Fig. 1(a)–(i), the wavefront of a plane wave becomes concave and convergent in the symmetric cuboid particle (pink auxiliary lines), leading to the formation of a typical photonic jet in the background medium. An asymmetric particle assembled by a cuboid of the same size and a wedge prism with  $\alpha = 18.43^\circ$  [ $\arctan(1/3)$ ] are illuminated by a plane wave, as shown in Fig. 1(a)–(ii). Here, the prism not only lets the photonic jet shift away from the optical axis, but also bends it in the central propagation, forming a “hook” shape. The peak  $E^2$  enhancement of the photonic hook reaches 12.9 in Fig. 1(a)–(ii), which is larger than the

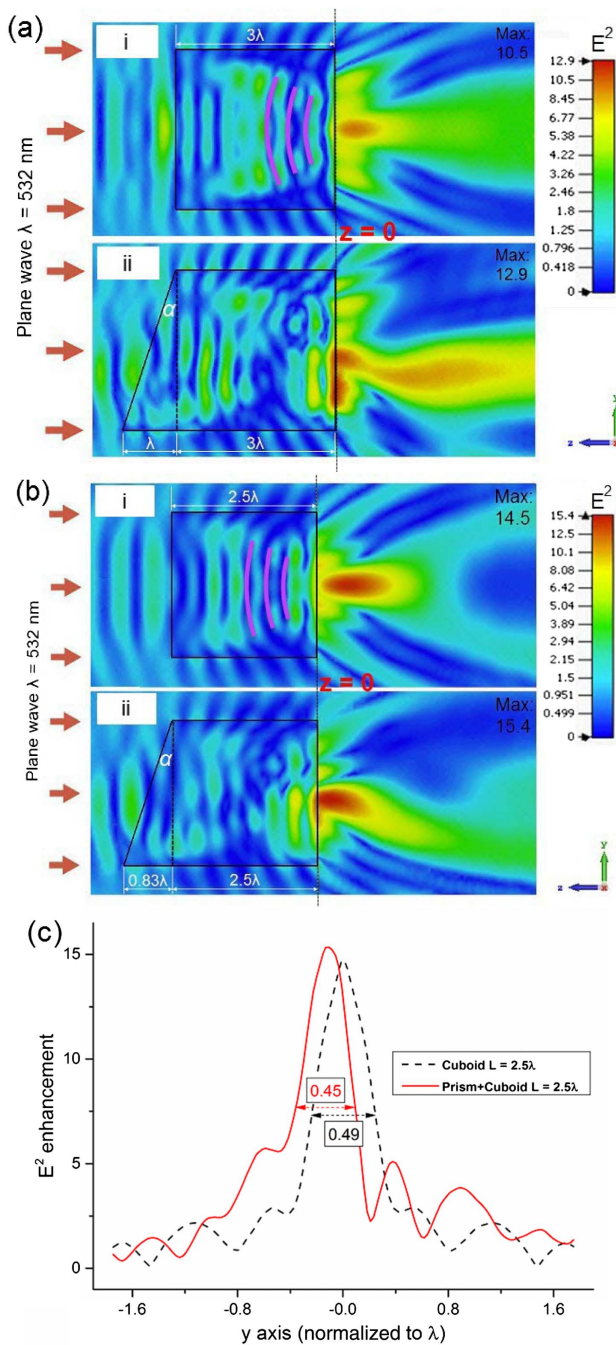


**Fig. 1.**  $E^2$  field intensity distribution for (a)  $L = 3\lambda$  and (b)  $L = 2.5\lambda$ . (c)  $E^2$  enhancement profiles along the  $y$ -axis for the symmetric and asymmetric particles with  $L = 2.5\lambda$ .

10.4 achieved by the jet from a normal cuboid particle exhibited in Fig. 1(a)–(i). The same “photonic hook” effect also appears in the asymmetric particle of a different size, as shown in Fig. 1(b)–(ii), where  $L = 2.5\lambda$  and  $\alpha = 18.43^\circ$  [ $\arctan(1/3)$ ]. In this case, the intensity enhancement of the photonic hook is larger than that achieved in Fig. 1(a)–(ii), reaching 15.4, and the high-intensity area is more concentrated around the bottom surface of the particle (right side), as shown in Fig. 1(b)–(ii). Figure 1(c) expresses the  $E^2$  enhancement profiles along the polarization direction ( $y$ -axis direction) for the positions

delivering maximum enhancements in the models of the symmetric and asymmetric particles with  $L = 2.5\lambda$ , demonstrated in Fig. 1(b). [ $z = 0$  is set to the flat end of the particle, as shown in Figs. 1(a) and 1(b), position  $z = -289.7$  for a symmetric model, and position  $z = -112.4$  for an asymmetric model.] It is shown that that the FWHM of the photonic hook (solid red curve) is shorter than that for the photonic jet induced by the symmetric cuboid particle (dashed black curve), and is able to break the simplified diffraction limit ( $0.5\lambda$  criterion).

The curvature of a photonic hook is defined by the factor  $\beta$  aided by a midline  $L_{\text{jet}}$ , and is the angle between the two lines linking the start point with the inflection point, and the inflection point with the end point of photonic hook, respectively, as shown in Fig. 2(a). To quantify the influence of the prism shape, we build several models, including an  $L = 3\lambda$  cuboid coupled with a variety of prisms with different  $\alpha$  values. Figure 2(b) summarizes the hook curvature— $\beta$  (degree, black curve—square markers) and the increase of the peak field enhancement (% , red curve—circle markers) compared to those in the symmetric cuboid case. The  $E^2$  distributions at several key  $\alpha$  values are illustrated in the insets in Fig. 2(b) to reveal the curvature changes of the photonic hooks. The symmetric cuboid represented as  $\alpha = 0^\circ$ , creates  $0^\circ$  for factor  $\beta$  and 0% for an increase of the peak field enhancement in Fig. 2(b), and a typical photonic jet from the cuboid particle can be seen in inset 1. When angle  $\alpha$  is increased from  $0^\circ$  to  $4.76^\circ$ , inset 2, the symmetry of the jet becomes broken, and the jet starts leaning to the direction of the longer side of the asymmetric particle ( $-y$  direction in our model), resulting in a  $7^\circ$   $\beta$  factor. The largest curvature,  $\beta = 35^\circ$ , is achieved at  $\alpha = 18.43^\circ$ , as shown in inset 3. However, a further increase of angle  $\alpha$  leads to the decrease of the curvature  $\beta$  factor, until almost  $\beta = 0^\circ$  at  $\alpha = 33.69^\circ$ . Inset 4 indicates the regression of  $\beta$  at a large  $\alpha$  angle, and the corresponding intensity enhancement distribution is characterized as a noncurved jet leaning towards the  $-y$  direction, where the start point, the inflection point, and the

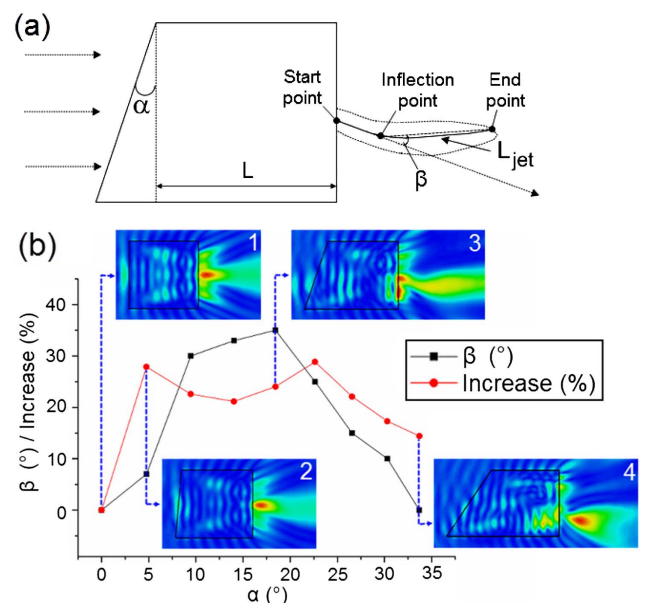


**Fig. 2.** (a) Diagram of photonic hook. (b) Curvatures and intensity enhancements for different  $\alpha$ .

end point of the jet form an almost straight line. In addition, an increase of the peak intensity enhancement exists in all asymmetric models, and a maximal 28.85% increase is obtained at  $\alpha = 22.62^\circ$ .

Traditionally, the generation of a strongly confined photonic jet depends on the trade-off between the refractive index contrast (dielectric particle to background media) and the scaling effect of the dielectric particle (relative-to-wavelength size), rather than the particle shape [12]. Consequently, the focusing of light by particles with the high degree of spatial symmetry, e.g., spheres, cylinders, or disks, is easier to calculate based on the aforementioned conditions and classic Lorenz–Mie theory. However, the formation of a photonic jet through a cuboid particle is due to the phase delay along the wavefront, rather than the factors that govern the focusing by spherical or cylindrical particles [12]. It is represented as a concave and convergent wavefront in the cuboid, shown as the pink auxiliary lines in Figs. 1(a)–(i) and 1(b)–(i). In the asymmetric particles, upper and lower halves of the particle [ $+y$  and  $-y$  direction in Figs. 1(a)–(ii) and 1(b)–(ii)] have different thicknesses along the  $z$ -axis. The diversity of the thickness with an asymmetric particle produces an unequal phase of the transmitted plane wave which is perpendicular to the  $y$ -axis, resulting in the irregularly concave deformation of the wavefront inside the particle, leading to the formation of a photonic hook. A light beam with astigmatism is a similar case in the macro-scale to help understand this process [14]. Additionally, in inset 4 in Fig. 2(b), the large prism angle  $\alpha$  provides great contrast of the concave deformation between the upper and lower halves of the asymmetric particle. The low-thickness upper half of the particle is more similar to the normal cuboid and may not be able to affect and “correct” the jet back to the direction of the incident plane wave. However, this capability could be kept in the scenarios of a lower  $\alpha$  angle, as shown in insets 2 and 3 in Fig. 2(b).

Power flow distributions in the asymmetric particles with  $\alpha = 18.43^\circ$  and their vicinity are plotted in Figs. 3(a)–3(d) to analyze the mechanism of the photonic hook formation with the variation of sizes:  $L = 1\lambda$ ,  $2.5\lambda$ ,  $3\lambda$ , and  $4.5\lambda$ , respectively.

The vortices in the power flow are stable foci in the phase space [15], and the power flow couples to the other planes through the singular points at the center of the vortex [16]. In Fig. 3, we can find a transition of the “bending” characteristic for the high-intensity area. Figure 3(a)  $L = 1\lambda$  has very similar features with the model of a symmetric cuboid particle, characterized as a centered noncurved hot spot with symmetric streamlines. Curvature of the hot spot and asymmetry of streamlines gradually appear in the power flow distributions of the particles with characteristic sizes from  $2.5\lambda$  to  $4\lambda$ , as shown in Figs. 3(b) and 3(c). The longest and most defined photonic hook is found in Fig. 3(c) and produced by the particle with  $L = 3\lambda$ . If we enlarge the particle to  $L = 4.5\lambda$ , the hot spot will maintain a long shape, as shown in Fig. 3(d).

Based on the above power flow analysis, it is shown that the photonic hook is the curved area with strong field enhancement, as shown in Fig. 3. Most of the power flow distributions of the normally straight photonic jets only match the profile of the high-intensity area in the region where power flows just exit the particle [17]. However, the photonic hook reported in this Letter can entirely match the trend of power flows in a certain shadow region. Interference caused by the diversity of the particle thickness along the polarization direction produces some more singular points in the vicinity of the asymmetric particle, which induces the curvatures appearing at the streamlines. Asymmetric particles that are smaller than  $L = 2.5\lambda$  do not have enough volume to trigger the enormous difference in the phase velocity between the upper and lower halves of the particle and, thus, cannot create the photonic hook. In addition, it is shown that the location of photonic hook moves away from the shadow boundary of the particle with the increasing size of the particle in Fig. 3. In the case of the large particle, e.g., Fig. 3(d), the corresponding long transmission distance of the jet in the background medium weakens the influence of the phase delay and interference. This produces a high-intensity stripe, instead of a photonic hook. It should be noted that this hybrid property of the beam profile described above makes it suitable for the optical trapping applications in

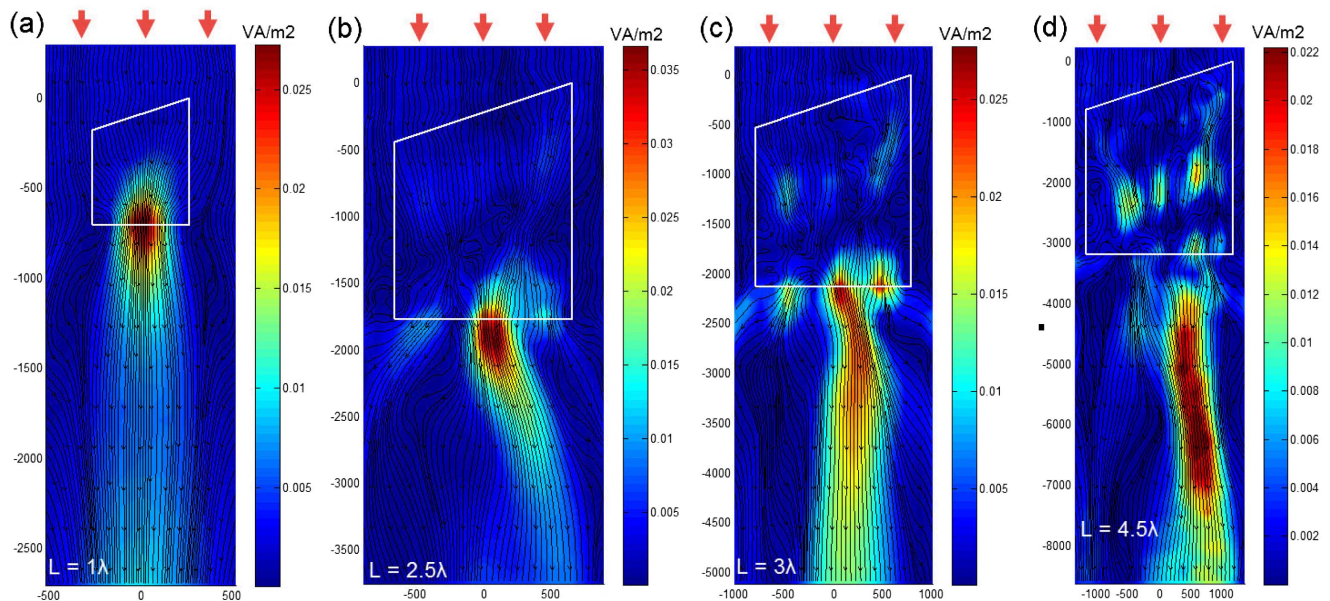


**Fig. 3.** Power flow diagrams for asymmetric particles  $L =$  (a)  $1\lambda$ , (b)  $2.5\lambda$ , (c)  $3\lambda$ , and (d)  $4.5\lambda$  with  $\alpha = 18.43^\circ$ .

mesoscale [18] and nanoscale [19–22] for the material and life science research.

In conclusion, the new type of curved light beam called the “photonic hook” is achieved via the numerical simulation of the focusing by an asymmetric dielectric particle, which is a cuboid topped with a wedge prism. It is shown that higher intensity and narrower focus can be offered by this photonic hook, compared to those of the jet produced by a normal cuboid lens. The power flow analysis of the scale models suggests that the photonic hook phenomenon is due to the unequal phase across the particle caused by the diversity of the particle thickness and the interference of local fields.

**Funding.** Sêr Cymru National Research Network in Advanced Engineering and Materials (NRN113, NRNF66); Knowledge Economy Skills Scholarships, KESS 2 (BUK289); the field distributions are calculated with the financial support of Russian Science Foundation (RSF) (16-52-00112, the principle of curved jet formation is developed with the partial financial support RSF 17-79-20051); Russian Fund for Basic Research (18-02-00414, 18-52-00005); Ministry of Education and Science of the Russian Federation (Minobrnauka) in the frame of GOSZADANIE (3.4982.2017/6.7); Mendeleev scientific fund of Tomsk State University (TSU); Tomsk Polytechnic University Competitiveness Enhancement Program grant.

## REFERENCES

1. M. V. Berry and N. L. Balázs, *Am. J. Phys.* **47**, 264 (1979).
2. G. A. Siviloglou, J. Broky, A. Dogariu, and D. N. Christodoulides, *Phys. Rev. Lett.* **99**, 213901 (2007).
3. N. K. Efremidis and I. D. Chremmos, *Opt. Lett.* **37**, 1277 (2012).
4. I. D. Chremmos and N. K. Efremidis, *Phys. Rev. A* **85**, 063830 (2012).
5. J. Broky, G. A. Siviloglou, A. Dogariu, and D. N. Christodoulides, *Opt. Express* **16**, 12880 (2008).
6. T. Vettenburg, H. I. C. Dalgarno, J. Nytk, C. Coll-Lladó, D. E. K. Ferrier, T. Čížmár, F. J. Gunn-Moore, and K. Dholakia, *Nat. Methods* **11**, 541 (2014).
7. D. N. Christodoulides, *Nat. Photonics* **2**, 652 (2008).
8. D. S. Benincasa, P. W. Barber, J. Zhang, W. Hsieh, and R. K. Chang, *Appl. Opt.* **26**, 1348 (1987).
9. A. Heifetz, S.-C. Kong, A. V. Sahakian, A. Taflove, and V. Backman, *J. Comput. Theor. Nanosci.* **6**, 1979 (2009).
10. Z. Chen, A. Taflove, and V. Backman, *Opt. Express* **12**, 1214 (2004).
11. B. S. Lukiyanchuk, R. Paniagua-Domínguez, I. V. Minin, O. V. Minin, and Z. B. Wang, *Opt. Mater. Express* **7**, 1820 (2017).
12. I. V. Minin and O. V. Minin, *Diffraction Optics and Nanophotonics: Resolution below the Diffraction Limit* (Springer, 2016).
13. I. H. Malitson, *J. Opt. Soc. Am.* **55**, 1205 (1965).
14. J. A. Arnaud and H. Kogelnik, *Appl. Opt.* **8**, 1687 (1969).
15. N. V. Karlov, N. A. Kirchenko, and B. S. Luk'yanchuk, *Laser Thermochemistry: Fundamentals and Applications* (Cambridge International Science, 2000).
16. Z. B. Wang, B. S. Luk'yanchuk, M. H. Hong, Y. Lin, and T. C. Chong, *Phys. Rev. B* **70**, 035418 (2004).
17. L. Yue, B. Yan, and Z. B. Wang, *Opt. Lett.* **41**, 1336 (2016).
18. I. V. Minin and O. V. Minin, “Device for forming the optical trap in the form of the photon hook,” Patent of Russia 161207 (27 October, 2015).
19. A. S. Shalin and S. V. Sukhov, *Plasmonics* **8**, 625 (2013).
20. A. S. Shalin, S. V. Sukhov, A. A. Bogdanov, P. A. Belov, and P. Ginzburg, *Phys. Rev. A* **91**, 063830 (2015).
21. A. A. Bogdanov, A. S. Shalin, and P. Ginzburg, *Sci. Rep.* **5**, 15846 (2015).
22. H. Xin, R. Xu, and B. Li, *Sci. Rep.* **2**, 818 (2012).